HHS Public Access

Author manuscript

Acta Biomater. Author manuscript; available in PMC 2017 August 04.

Published in final edited form as:

Acta Biomater. 2017 February ; 49: 140–151. doi:10.1016/j.actbio.2016.11.046.

Anatomical region-dependent enhancement of 3-dimensional chondrogenic differentiation of human mesenchymal stem cells by soluble meniscus extracellular matrix

Benjamin B. Rothrauff[a,b], **Kazunori Shimomura**[a,c], **Riccardo Gottardi**[a,d], **Peter G. Alexander**[a], and **Rocky S. Tuan**[a,b,*]

[a]Center for Cellular and Molecular Engineering, Department of Orthopaedic Surgery, University of Pittsburgh, Pittsburgh, PA 15219, U.S.A

[b]McGowan Institute for Regenerative Medicine, University of Pittsburgh, Pittsburgh, PA 15219, U.S.A

[c]Medicine for Sports and Performing Arts, Department of Health and Sport Sciences, Osaka University Graduate School of Medicine, Osaka 565-0871, Japan

[d]Fondazione RiMED, Italy

Abstract

Extracellular matrix (ECM) derived from decellularized tissues has been found to promote tissue neogenesis, most likely mediated by specific biochemical and physical signaling motifs that promote tissue-specific differentiation of progenitor cells. Decellularized ECM has been suggested to be efficacious for the repair of tissue injuries. However, decellularized meniscus contains a dense collagenous structure, which impedes cell seeding and infiltration and is not readily applicable for meniscus repair. In addition, the meniscus consists of two distinct anatomical regions that differ in vascularity and cellular phenotype. The purpose of this study was to explore the region-specific bioactivity of solubilized ECM derived from the inner and outer meniscal regions as determined in 2D and 3D cultures of adult mesenchymal stem cells (MSCs). When added as a medium supplement to 2D cultures of MSCs, urea-extracted fractions of the inner (imECM) and outer meniscal ECM (omECM) enhanced cell proliferation while imECM most strongly upregulated fibrochondrogenic differentiation on the basis of gene expression profiles. When added to 3D cultures of MSCs seeded in photocrosslinked methacrylated gelatin (GelMA)

*Corresponding author: Rocky S. Tuan, PhD, Center for Cellular and Molecular Engineering, Department of Orthopaedic Surgery, University of Pittsburgh School of Medicine, 450 Technology Drive, Room 221, Pittsburgh, PA, 15219, USA., Tel: +1 4126482603, Fax: +1 4126245544, rst13@pitt.edu.

Benjamin B. Rothrauff, PhD, 450 Technology Drive, Room 239, Pittsburgh, PA, 15219, USA, Phone: 4126245503, Fax: 4126245544, bbr4@pitt.edu

Kazunori Shimomura, MD, PhD, 2-2 Yamadaoka, Suita, Osaka 565-0871, Japan, Phone: 81662108439, Fax: 8162108438, kazunori-shimomura@umin.net

Riccardo Gottardi, PhD, 450 Technology Drive, Room 239, Pittsburgh, PA, 15219, USA, Phone: 4126245503, Fax: 4126245544, rig10@pitt.edu

Peter G. Alexander, PhD, 450 Technology Drive, Room 239, Pittsburgh, PA, 15219, USA, Phone: 4126245503, Fax: 4126245544, pea9@pitt.edu

Rocky S. Tuan, PhD, 450 Technology Drive, Room 239, Pittsburgh, PA, 15219, USA, Phone: 4126245503, Fax: 4126482603, rst13@pitt.edu

Disclosure Statement

No competing financial interests exist.

hydrogels, both ECM fractions upregulated chondrogenic differentiation as determined by gene expression and protein analyses, as well as elevated sulfated glycosaminoglycan sGAG content, compared to ECM-free controls. The chondrogenic effect at day 21 was most pronounced with imECM supplementation, but equivalent between ECM groups by day 42. Despite increased cartilage matrix, imECM and omECM constructs possessed compressive moduli similar to controls. In conclusion, soluble meniscal ECM may be considered for use as a tissue-specific reagent to enhance chondrogenesis for MSC-based 3D cartilage tissue engineering.

Keywords

Meniscus; Extracellular Matrix; Fibrochondrogenesis

1. Introduction

The menisci of the knee, crescent-shaped fibrocartilaginous tissues interposed between the articular surfaces of the femur and tibia, must resist compressive, tensile, and shear forces in order to efficiently distribute tibiofemoral contact stresses and maintain joint health [1, 2]. As with other musculoskeletal tissues, the complex structure of the meniscus imparts a unique function, allowing the meniscus to facilitate efficient articulation of the tibiofemoral joint. A gradient of decreasing collagen type II and proteoglycan content exists when moving from inner meniscal regions towards the periphery, while the outer region is principally composed of aligned collagen type I fibers capable of resisting hoop stresses arising from joint loading [3–7]. Much like hyaline cartilage, the inner region of the meniscus is avascular, while blood vessels infiltrate the outer 10–30% of the meniscus width [8]. The region-specific differences in ultrastructure and biochemical composition correspond to differences in cell phenotype; inner meniscal cells possess a round morphology reminiscent of articular chondrocytes while cells of the outer meniscus are found between aligned collagen fibers, similar to fibroblasts of tendon or ligament [1, 2]. Similarly, cells of the inner region express higher levels of collagen type II and aggrecan while cells of the outer region express greater collagen type I [9].

Given the rapid onset of joint degeneration experienced with the loss of meniscal function [10, 11], coupled with the limited availability and narrow inclusion criteria associated with meniscal allograft transplantation, tissue engineers have sought to develop novel biomaterials to serve as a meniscus substitute [12, 13]. Decellularized menisci derived from animal sources have been explored, as the removal of cellular material could mitigate an adverse immune response while preservation of tissue ultrastructure and biochemical composition could maintain meniscal function and promote region-specific differentiation of infiltrating host cells. However, the dense collagenous extracellular matrix (ECM) of native menisci necessitates relatively harsh decellularization protocols with resulting losses in proteoglycan content and the associated compressive moduli of inner meniscal regions [14, 15]. Despite these alterations in ultrastructural and biochemical properties, infiltration of seeded cells is still limited [16, 17].

Enzymatic digestion (e.g., pepsin) of decellularized meniscus ECM can produce a thermoresponsive hydrogel capable of delivering exogenous cells to a meniscal lesion, while theoretically retaining meniscus-specific bioactive motifs capable of directing fibrocartilaginous neotissue formation [18]. However, Lin et al. [19] reported that pepsin digestion of ECMs offered negligible advantage over collagen type I in terms of promoting proliferation, migration, and multilineage differentiation of mesenchymal stem cells (MSCs), likely due to the proteolytic removal of functional components. On the other hand, a urea-soluble fraction of ECM has been demonstrated in several studies to promote differentiation of MSCs towards tissue-specific (i.e., homologous) phenotypes [19–21]. Most recently, we demonstrated that urea-soluble extracts of the inner and outer meniscus ECM could promote region-specific gene expression of MSCs seeded in a photocrosslinked polyethylene glycol diacrylate (PEGDA) hydrogel [22]. Expanding on these findings, this study explores the effect of urea-soluble extracts of the inner and outer meniscus ECM in promoting chondrogenic/fibrochondrogenic differentiation of MSCs seeded in a visible light (VL) photocrosslinked methacrylated gelatin (GelMA) hydrogel. GelMA hydrogels have been shown to support robust chondrogenesis of encapsulated MSCs [23] while the use of a VL-activated photoinitiator obviates concerns of UV light-induced mutagenesis or cytotoxicity [24]. We hypothesized that the ECM extracts would promote region-specific cell phenotypes, with the inner and outer ECM extracts respectively enhancing chondrogenic and fibrochondrogenic differentiation of MSCs seeded in GelMA hydrogels.

2. Methods

2.1. Overview of experimental design

Urea-soluble extracts from the decellularized ECM of inner and outer regions of juvenile bovine menisci were isolated and characterized. The biological effects of ECM extracts on human bone marrow MSCs were evaluated in both 2D and 3D cultures in vitro. MSCs were cultured on 2D plastic in the presence of ECM-supplemented media; assays for cell morphology, metabolism, and gene expression were performed up to 7 days of culture. For 3D constructs, MSCs were encapsulated in ECM-enhanced GelMA hydrogels and cultured for up to 42 days to assess the region-specific bioactivity of the ECM extracts, as evaluated on the basis of gene expression, histology, immunohistochemistry, biochemical composition, and mechanical properties.

2.2. Meniscus ECM preparation

2.2.1. ECM decellularization—Menisci were procured from hindlimbs of 6–8 week old cows (Research 87, Boylston, MA) and stored in a protease inhibitor solution (phosphate-buffered saline, PBS; 5 mM ethylenediaminetetraacetic acid, EDTA; 0.5 mM phenylmethylsulfonyl fluoride, PMSF) at −20°C until use. Once thawed, menisci were halved, coarsely minced (Fig. 1A–C), and decellularized by adapting a previously established method [21]. Briefly, 4 g of minced tissue was agitated for 24 hours at 4°C in 40 ml of protease inhibitor solution containing 1% Triton X-100 (Sigma-Aldrich, St. Louis, MO, USA), followed by 3 washes (30 minutes each at 4°C) in PBS. Subsequently, 40 ml of Hanks Buffered Salt Solution (HBSS, Thermo Fisher Scientific, Pittsburgh, PA, USA) supplemented with 200 U/ml DNase and 50 U/ml RNase (Worthington, Lakewood, NJ,

USA) was added to the tissue, with continuous agitation for 12 hours at room temperature. The tissue was washed six times in PBS, as above, before freezing and subsequent lyophilization. Native and decellularized tissues were evaluated for histological appearance, cellular content, and biochemical composition, including total collagen and sulfated glycosaminoglycan (sGAG) contents, as described below.

2.2.2. Histology of native and decellularized ECM—Native and decellularized tissues were fixed in 10% phosphate-buffered formalin, serially dehydrated, embedded in paraffin, and then sectioned (6 μm thickness) with a microtome (Leica RM2255, Leica Biosystems, Buffalo Grove, IL, USA). Samples were rehydrated and stained with haematoxylin & eosin (H&E, Sigma-Aldrich) or 4′,6-diamidino-2-phenylindole, dilactate (DAPI, Life Technologies, Carlsbad, CA, USA). H&E-stained samples were imaged using an Olympus SZX16 stereo microscope while DAPI-stained sections were examined with an Olympus CKX41 inverted microscope using fluorescent excitation at 405 nm.

2.2.3. Biochemical composition of native and decellularized ECM—To determine the biochemical composition of native and decellularized tissues, dried samples were digested overnight at 65°C at a concentration of 10 mg/mL in a digestion buffer (pH 6.0) containing 2% papain (v/v, from Papaya latex, Sigma-Aldrich), 0.1 M sodium acetate, 0.01 M cysteine HCl, and 0.05 M EDTA. The pH was then adjusted to 7.0 through addition of concentrated NaOH. sGAG content was quantified with a Blyscan Assay according to the manufacturer's instructions (Biocolor, Carrickfergus, United Kingdom). dsDNA content was determined using the Quant-iT Picogreen dsDNA assay (Life Technologies). Total collagen content was determined using a modified hydroxyproline assay. Briefly, 200 μL of each sample was hydrolyzed with an equal volume of 4 N NaOH at 121°C for 75 min, neutralized with an equal volume of 4 N HCl, and then titrated to an approximate pH of 7.0. The resulting solution was combined with 1.2 mL chloramine-T (14.1 g/L) in buffer (50 g/L citric acid, 120 g/L sodium acetate trihydrate, 34 g/L NaOH, and 12.5 g/L acetic acid) and allowed to stand at room temperature for 30 min. The solution was then combined with 1.2 mL of 1.17 mM p-dimethylaminobenzaldehyde in perchloric acid and placed in a 65°C water bath for 20 minutes. 200 μL of each sample was added to a clear 96-well plate, in duplicate, and absorbance at 550 nm was read. PureCol bovine collagen (3.2 mg/mL, Advanced Biomatrix, Carlsbad, CA, USA) was serially diluted to provide a standard curve ranging from 0 to 1000 μg/mL.

2.2.4. Solubilization of decellularized ECM—Decellularized tissues were cryomilled into a fine powder (Spex Freezer Mill 8670, Metuchen, NJ, USA) and urea-soluble extracts of the decellularized ECM of inner and outer meniscal regions were obtained using a previously described method (Fig. 1D, E) [21]. Briefly, 4 g of wet decellularized ECM powder was agitated for 3 days at 4°C in 40 mL of 3 M urea dissolved in water. The suspension was centrifuged for 20 minutes at 1,500g and the supernatant was transferred to benzoylated dialysis tubing (Sigma-Aldrich) and dialyzed against ddH_2O for 2 days at 4°C, changing the water every 8 hours. The dialyzed ECM extract was transferred to centrifugal filter tubes (3000 MWCO; EMD Millipore, Billerica, MA, USA) and spin-concentrated approximately 10-fold at 1,500g for 60 minutes. The final ECM extract was filter-sterilized

through a PVDF syringe filter unit (0.22 μm; EMD Millipore). Protein concentration was determined by BCA assay (Thermo Fisher Scientific) and aliquots of 1,000 μg/mL were stored at −80°C until further use. Before use in experimental studies, aliquots prepared from three different batches were pooled.

In preliminary studies, decellularized ECM was alternatively solubilized by pepsin digestion using an established protocol [25, 26]. In particular, ECM powders were enzymatically digested in a solution of 1 mg/mL porcine pepsin (Sigma-Aldrich) in 0.01 N HCl for 48 hours at room temperature under continuous stirring. The resulting ECM slurries (Fig. 1F) were neutralized by addition of one-tenth digest volume of 0.1 N NaOH and one-ninth digest volume of 10X PBS, then further diluted by addition of PBS. These pepsin-solubilized ECM hydrogels (i.e., imAP, omAP) were principally composed of collagen (Fig. 1G, H) and were inferior to urea-soluble extracts in promoting cell proliferation and fibrochondrogenic differentiation (data not shown); they were therefore excluded from additional experiments.

2.2.5. SDS-PAGE and growth factor analysis of ECM—Dried samples of native inner and outer meniscus ECM, and their corresponding urea-soluble and pepsin-digested extracts were suspended in TM buffer (Total Protein Extraction Kit, EMD Millipore). 30 μg total protein was mixed with SDS loading buffer and reducing agent (NuPAGE; Life Technologies, Carlsbad, CA, USA) and heated for 10 minutes at 70°C. Protein was loaded into a pre-cast 10-well NuPAGE 4–12% Bis-tris Minigel (Life Technologies) and separated by electrophoresis in MOPS running buffer for 50 minute at constant 200V. The gel was washed several times in water and photographed using a CCD camera gel imaging system (FOTODYNE, Hartland, WI, USA).

Additionally, the growth factor contents of the urea-soluble extracts of the inner meniscus (imECM) and outer meniscus (omECM) were measured using a Human Growth Factor Array (RayBiotech, Norcross, GA), according to the manufacturer's instructions.

2.3 Bioactivity of meniscus ECM extract in 2-dimensional cell culture

Human bone marrow MSCs were obtained as previously described [19]. All experiments were performed with passage 3 (P3) MSCs pooled from 3 patients (31 year old female, 42 year old male, 44 year old male) undergoing total hip arthroplasty with Institutional Review Board approval (University of Washington and University of Pittsburgh). To determine the effect of ECM extracts on MSC morphology and metabolism, cells were suspended in growth medium (DMEM, 10% FBS, 1% Anti-Anti; Life Technologies) and plated in 6-well culture plates at a density of 1×10^3 cells/cm^2. One day following cell seeding, growth medium was replaced with serum-free medium (DMEM, 1% antibiotic-antimycotic, 1% Insulin-transferrin-selenium [ITS]; Life Technologies) with or without ECM extract supplementation. There were three media conditions – (1) serum-free control, (2) supplementation with 50 μg/ml imECM, and (3) supplementation with 50 μg/ml omECM. Media were changed every 2 days. On days 1, 3, and 7, an MTS assay (CellTiter 96® AQ_{ueous} Non-Radioactive Cell Proliferation Assay; Promega, Madison, WI) was performed according to manufacturer's instructions.

To determine the effects of ECM extracts on gene expression, 2×10^4 cells/cm^2 were plated in 6-well culture plates and cultured for up to 7 days, as described above. On days 1, 3, and 7, total RNA was isolated from cells using an RNeasy Plus Mini Kit (Qiagen, Valencia, CA, USA) and reverse transcribed into cDNA through use of SuperScript III first-strand synthesis kit (ThermoFisher Scientific, Pittsburgh, PA, USA). Quantitative real-time polymerase chain reaction (qPCR) was performed using SYBR® Green master mix (Applied Biosystems, Foster City, CA) on a StepOnePlus Real-Time PCR system (Applied Biosystems). Relative expression of each target was calculated using the $\Delta\Delta C_T$ method with the arithmetic average of GAPDH and 18S rRNA expression used as the endogenous reference. For 2D cultures, expression of SOX9, collagen type II (COL2), collagen type I (COL1), aggrecan (ACAN), and RUNX2, was analyzed. Additional targets were included for 3D cultures, as described below. Primer sequences are listed in Supplemental Table 1. As significant differences across treatment groups were only seen at day 3, expression levels were normalized against day 3 controls.

2.4. Bioactivity of meniscus ECM extract in 3-dimensional GelMA hydrogels

Methacrylated gelatin (GelMA) was prepared as previously described [23]. ECM-enhanced GelMA contained 500 μg/mL of imECM or omECM, whereas controls were supplemented with an equal volume of PBS. MSCs were suspended in the liquid GelMA (8% w/v suspended in HBSS with 0.2% v/v of visible light-sensitive photoinitiator lithium phenyl-2,4,6-trimethylbenzoylphosphinate, LAP) at 15×10^6 cells/mL. 50 μL of the cell suspension was distributed to silicone molds measuring 5 mm diameter × 2 mm depth and exposed to high intensity visible light (450–490 nm) for 2 minutes to induce photogelation. MSC-encapsulated hydrogels were transferred to 6-well plates previously coated with silicone (Sigmacote, Sigma-Aldrich) to prevent cell migration and adhesion onto the plastic surface, and cultured for up to 42 days in full chondrogenic medium (DMEM, 1% antibiotic-antimycotic, 1% ITS, 0.1 μM dexamethasone, 40 μg/mL proline, 50 μg/mL ascorbate-2-phopshate, 10 ng/mL recombinant human transforming growth factor β3 [TGF-β3; Peprotech, Rocky Hill, NJ, USA]). Medium was changed every 2–3 days. The MSC-encapsulated hydrogels were collected at various time points and analyses for gene expression, biochemical composition, histology and immunohistochemistry, and compressive mechanical properties, were performed.

2.4.1. Gene expression and biochemical composition analyses—On days 1, 7, 21, and 42, total RNA was isolated from constructs through sequential use of Trizol (Thermo Fisher Scientific) and RNeasy Plus Mini Kit (Qiagen), according to manufacturers' protocols. Reverse transcription and qPCR was performed as described above. Expression of the following gene targets was determined for the 3D constructs – SOX9, collagen type II (COL2), collagen type I (COL1), aggrecan (ACAN), collagen type VI (COL6), RUNX2, cartilage oligomeric matrix protein (COMP), platelet-derived growth factor receptor (PDGFR), tissue inhibitor of metalloproteinase 2 (TIMP2), scleraxis (SCX), tenascin C (TNC), and fibromodulin (FMOD). Relative expression of each condition at a given time point was normalized against day 1 controls. Primer sequences are listed in Supplemental Table 1.

On days 21 and 42, constructs were digested overnight in papain using the protocol described in *Section 2.2.3*. Total sGAG and dsDNA contents were determined, allowing subsequent normalization of sGAG by dsDNA.

2.4.2. Histological and immunohistochemical analysis—Histological sections were prepared on days 21 and 42 following a similar protocol as performed when characterizing the appearance of native and decellularized meniscal tissues described in *Section 2.2.2*. Following rehydration, samples were stained with Safranin O/Fast Green (Electron Microscopy Sciences, Hatfield, PA USA); nuclei were counterstained with Hematoxylin. For immunohistochemical staining of collagens type II and type I, antigen retrieval was achieved by incubation of slides for 30 minutes at 37°C in Chondroitinase ABC (100mU/ml, Sigma) and Hyaluronidase (250 U/ml, Sigma) suspended in 0.02% bovine serum albumin (BSA). Endogenous peroxidase activity was blocked with 3% H_2O_2 (in methanol). Non-specific binding was blocked with 1% horse serum. Samples were then exposed to rabbit anti-human collagen type II primary antibody (ab34712; Abcam, Cambridge, MA, USA) diluted 1:400 or rabbit anti-human collagen type I primary antibody (ab34710; Abcam) diluted 1:100 in 1% horse serum overnight at 4°C. Equine biotinylated secondary antibody binding, signal amplification, and visualization were achieved through the use of VectaStain Universal Elite ABC Kit (Vector Laboratories, Burlingame, CA, USA) in accordance with the manufacturer's instructions. Nuclei were counterstained with Haematoxylin QS (Vector).

2.4.3. Compressive mechanical testing—On day 42, the cylindrical specimens were tested in uniaxial unconfined compression with a Bose Electroforce 3200 series II (resolution 1nm, load cell 1000g) while kept moist in PBS. After a preload condition of 0.1% strain, samples were compressed at a 0.01 mm/s rate reaching a strain of 20%. The elastic modulus E was extracted by linear fitting of the final part of the stress-strain curve near the maximum load as previously described [7].

2.5. Statistical analyses

Comparisons across multiple conditions or time points were made using a one-way or two-way analysis of variance (ANOVA) with Tukey post-hoc testing for multiple comparisons. When comparing two conditions, a Student's t-test was performed. Data are presented as mean ± standard deviation. Sample sizes are indicated in figure legends. Statistical significance was considered $p < 0.05$.

3. Results

3.1. Characterization of inner and outer meniscal ECM

Histological staining confirmed the absence of cell nuclei in both inner and outer meniscal ECM prepared by the decellularization protocol (Fig. 2A–H), with a corresponding reduction in dsDNA content (Fig. 2I; Native vs. Decellularized – Inner: 555.1 ± 62.5 ng/mg vs. 7.7 ± 6.2 ng/mg, $p < 0.001$; Outer: 616.3 ± 52.1 ng/mg vs. 11.7 ± 9.4 ng/mg, $p < 0.001$). Decellularized ECM from both inner and outer regions possessed a lower sGAG content than the respective native tissues ($p < 0.001$). However, native and decellularized inner meniscal ECM possessed higher sGAG content (31.7 ± 6.8 μg/mg and 9.7 ± 5.9 μg/mg,

respectively) than outer meniscal ECM (10.0 ± 1.7 μg/mg and 1.6 ± 1.0 μg/mg, respectively) at the corresponding step (Fig. 2J). Conversely, the total collagen content was equivalent between meniscal regions and remained constant following decellularization (Fig. 2K). As compared to native inner and outer meniscus, imECM and omECM possessed a reduced amount of high molecular weight proteins, including collagen, but relatively more abundant low and moderate molecular weight proteins and/or fragments, as seen by SDS-PAGE (Fig. 1G, H). Growth factor array analysis revealed differences in several proteins when comparing imECM with omECM; notably, basic fibroblast group factor (bFGF) was found only in omECM while TGF-β concentrations were higher in imECM (Table 1).

3.2. ECM-induced MSC proliferation and fibrochondrogenic differentiation in 2D culture

Over a 7-day culture period, imECM and omECM exposure enhanced cell proliferation of MSCs as observed by phase contrast microscopy (Fig. 3A–C) and MTS assay. imECM and omECM supplementation increased cell proliferation equivalently at all time points (Fig. 3D). On day 3, both imECM and omECM increased expression of SOX9, COL2, and COL1, although statistically significant increases over controls were only seen with imECM supplementation ($p < 0.05$). ACAN and RUNX2 expression did not significantly differ across conditions.

3.3. Gene expression of 3D MSC cultures in GelMA hydrogels enhanced with ECM

Seeding of MSCs in GelMA hydrogels supported robust upregulation of cartilage matrix genes, COL2 and ACAN, over a 42-day culture, with modest increases in COL1 and RUNX2 expression in all groups on days 7 and 21, before returning to baseline on day 42 (Fig. 4). imECM exposure upregulated SOX9 over controls and omECM on day 1, while both ECM groups were slightly inferior to controls on day 7 before demonstrating equivalency across groups at later time points. Both ECM groups strongly upregulated COL2 expression on day 7, while only imECM supplementation maintained enhanced expression over controls on day 21. Conversely, omECM upregulated COL1 expression on day 1, while both imECM and omECM had significantly reduced COL1 expression on day 21 compared to controls. imECM and omECM increased ACAN expression on day 21, but differences were not statistically significant. COL6 expression across all groups was downregulated after day 1, with further reductions induced by omECM on days 7 and 21. RUNX2 expression was decreased in omECM and imECM constructs on days 7 and 42, respectively, as compared with controls. Expression of additional genes associated with the fibrochondrocyte and fibroblast phenotypes was measured (Supplemental Fig. 1), showing that ECM supplementation had either a negligible or inhibitory effect as compared against controls.

3.4. Immunohistochemical and histological staining of MSC-seeded GelMA constructs

At day 21, positive staining for collagen type II was found in the pericellular region, with cells near the construct perimeter demonstrating more intense staining (Fig. 5A–F). ECM-supplemented constructs exhibited greater collagen type II deposition, with imECM constructs superior to omECM constructs. By day 42, all groups demonstrated robust collagen type II immunostaining distributed throughout the entire construct area (Fig. 5G–L). In comparison, regions of reduced intensity were found between intensely staining

clusters only in Controls, while imECM and omEMC constructs exhibited a more homogeneous distribution of intense collagen type II staining.

Proteoglycan deposition, as visualized through Safranin O staining, paralleled collagen type II immunostaining (Fig. 6). Both imECM and omECM constructs showed more intense staining on day 21, as compared to Controls, with imECM producing the greatest effect (Fig. 6A–F). However, by day 42, all constructs showed intense proteoglycan deposition and differences among groups could not be qualitatively detected (Fig. 6G–L). Supplementation of the culture medium with TGF-β3 was essential for such robust anabolic effects. When constructs were cultured in the absence of TGF-β3, no proteoglycan deposition was noted in Controls by day 42 (Supplemental Fig. 2A, F). Inclusion of imECM and omECM within hydrogels only resulted in low levels of pericellular proteoglycan deposition (Supplemental Fig. 2B–C, G–H), but staining intensity was much less that of constructs cultured in TGF-β3 containing full chondrogenic medium (Fig. 6). Acellular constructs, even with ECM supplementation, were negative for proteoglycan deposition (data not shown), supporting the cellular origin of the histologically detectable proteoglycan.

Immunohistochemical staining for collagen type I showed a pattern opposite to that seen for collagen type II and proteoglycan (Fig. 7). In particular, imECM constructs showed the least collagen type I deposition on days 21 and 42. Controls and omECM constructs showed comparable collagen type I deposition on day 21 (Fig. 7A–F), but by day 42, staining intensity was most profound in Controls (Fig. 7G–L).

3.5. Biochemical composition and compressive moduli of MSC-seeded GelMA hydrogels

The biochemical composition of constructs mirrored the histological findings. Total sGAG content was significantly increased in imECM and omECM constructs on days 21 and 42 (Fig. 8A), while no significant difference in dsDNA content was found over time or among groups (Fig. 8B). Nevertheless, when sGAG content was normalized to cellular content, only imECM constructs showed significantly elevated values over Controls on day 21, while both ECM-supplemented groups were significantly increased by day 42 (Fig. 8C). Similar to the histological findings, acellular constructs possessed negligible sGAG content, even when supplemented with imECM or omECM (data not shown); imECM and omECM constructs trended towards higher compressive moduli than Controls, but these differences were not statistically significant (Fig. 8D).

4. Discussion

Expanding on our recent work [22], this study investigated the region-specific bioactivity of urea-extracted decellularized meniscal ECM when presented to human bone marrow MSCs in both 2D and 3D cultures. In preliminary studies, pepsin-digested hydrogels derived from decellularized inner and outer meniscal ECM did not affect fibrochondrogenic differentiation of MSCs when added as a medium supplement in 2D culture or when seeded with MSCs as a 3D hydrogel. The absence of fibrochondroinductivity of pepsin-digested hydrogels agrees with recent work by Visser et al. [27] which showed the supplementation of pepsin-soluble meniscal ECM to MSCs in hydrogel cultures did not alter gene expression or protein deposition. As seen both grossly and by SDS-PAGE, pepsin digestion yielded a

slurry that contains predominantly collagen. Conversely, urea-extracted fractions are enriched for low to moderate molecular weight proteins, the combination of which has been previously demonstrated to promote tissue- or region-specific differentiation of MSCs [19–22]. Similarly, in this study, imECM and omECM were found to promote MSC proliferation and upregulation of fibrochondrogenic markers SOX9, COL2, and COL1, when added as a supplement in 2D culture. Based upon these findings, the bioactivities of imECM and omECM were further explored when mixed with MSC-seeded GelMA hydrogels.

GelMA is a versatile biomaterial capable of supporting robust chondrogenic differentiation of encapsulated MSCs after rapid light-activated gelation [23, 28]. Additionally, the inclusion of a water-soluble, visible light-responsive photoinitiator (i.e., LAP) obviates concerns of possible cellular damage caused by UV light exposure, as required by most photoinitiators (e.g., Irgacure) [24]. While the effect of meniscal ECM supplementation on MSC-seeded GelMA hydrogels was previously unexplored, functionalization of GelMA with particulated (hyaline) cartilage ECM has been reported to enhance chondrogenesis of encapsulated MSCs [29, 30]. Although the particulated ECM was presumably chondroinductive due to retention of intrinsic chondrogenic cues, robust chondrogenesis required stimulation with exogenous TGF-β3. A similar result was found in this study. Namely, imECM and omECM supplementation of MSC-GelMA constructs produced discernible low-level deposition of proteoglycan in the pericellular regions when cultured in medium without TGF-β3 (Supplemental Fig. 2), but modestly upregulated expression of chondrogenic markers (data not shown). In contrast, additional supplementation of TGF-β3 to culture medium produced robust chondrogenic differentiation of MSCs, as determined by multiple assays. Supplementation with meniscal ECM enhanced chondrogenic gene expression at earlier time points (i.e., days 7 and 21), translating into sustained increases in collagen type II and sGAG deposition at days 21 and 42. While omECM supplementation significantly upregulated COL1 expression on day 1, the effect was not sustained over the culture period. Rather, constructs supplemented with either imECM or omECM demonstrated repressed COL1 expression at day 21, as compared against Controls. Similarly, ECM-mediated decrements in collagen type I deposition were seen on day 42 by immunohistochemistry. In our previous study [22], in which PEGDA hydrogels were supplemented with inner or outer meniscal ECM, omECM constructs showed sustained upregulation of COL1 expression for at least 7 days while imECM preferentially upregulated COL2 expression, suggesting region-specific bioactivity of the soluble meniscal ECM. However, later time points were not included nor was immunohistochemical staining performed, as employed in this study, which showed both imECM and omECM similarly enhanced chondrogenesis by day 42. Although the mechanistic basis underlying these discrepancies between studies in not presently clear, differences in hydrogel composition (i.e., GelMA vs. PEGDA), cell densities (i.e., 15.0×10^6 vs. 1.0×10^6 MSCs/mL), meniscal ECM-hydrogel interactions, cell adhesion/morphology, and duration of TGF-β3 exposure, may have contributed to the relatively equivalency of chondrogenic bioactivity of imECM and omECM supplements. More specifically, the prolonged exposure to TGF-β3 in the culture medium may have saturated the independent chondrogenic bioactivity mediated by soluble meniscal ECM.

For instance, imECM transiently upregulated expression of chondrogenic regulator SOX9 on day 1, with negligible differences across groups at later time points. Interestingly, cells isolated from the inner and outer regions of native menisci were reported to express equivalent levels of SOX9, suggesting minimal influence of SOX9 in distinguishing region-specific phenotypes [9]. Vanderploeg et al. [6] showed collagen type VI to be concentrated in inner meniscal regions and localized to the pericellular matrix; in this study, omECM supplementation downregulated Col6 expression, as compared with Controls and imECM constructs. In examining additional putative meniscal cell markers [31], ECM supplementation tended to have a negligible or inhibitory effect at early time points, with broad equivalency across groups by day 42. The extent that these transcriptional changes are meaningful for tissue engineering application remains uncertain, given the paucity of studies characterizing the phenotypes of cells across various meniscus regions.

On the other hand, the homogeneous distribution of MSCs within GelMA hydrogels clearly does not recapitulate the complex fibrous architecture of native menisci [1, 2]. In particular, tie fibers are known to extend radially from the central meniscus to the periphery, binding aligned circumferential fibers and allowing efficient transformation of compressive loads into hoop stresses [1]. In an in vitro model, Puetzer and Bonassar [32] demonstrated that simulated tibiofemoral loading of an engineered meniscus composed of high density collagen seeded with meniscal fibrochondrocytes began to recapitulate the fibrous ultrastructure and resulting mechanical anisotropy of native menisci. Whether mechanical loading could orchestrate similar structural organization of MSC-GelMA constructs remains to be explored.

Alternatively, ECM-supplemented hydrogels may be combined with electrospun nanofibers to better reconstitute the structural and biochemical properties of the meniscus [33, 34]. Baek et al. [35] fabricated multilayered scaffolds with alternating layers of electrospun nanofibers and MSC-seeded alginate hydrogels, which allowed tunable tensile anisotropy depending on fiber orientation. However, compressive mechanical properties were not measured. In this study, compressive moduli of constructs (~ 40–50 kPa) did not differ across groups. These values are weaker than those of native menisci (~ 100–500 kPa) [2, 36, 37] but few studies have examined the differences between compressive properties of the inner and outer meniscal regions. On the other hand, the modulus values found herein are congruent with reported values for GelMA hydrogels [23, 38]. Unlike other studies, in which values of compressive modulus correlated with glycosaminoglycan content [38, 39], the greater sGAG content of ECM-supplemented constructs did not significantly enhance compressive moduli, suggesting that the differences in sGAG content or the resulting hydrogel architecture were insufficient to produce discernible changes in mechanical properties. Analyses of possible ECM-mediated increases in collagen content were not performed, as the gelatinous nature of the GelMA hydrogel would likely obscure any group differences.

As with fiber architecture, mechanical loading has been found to further increase sGAG deposition, with concurrent improvements in compressive mechanical properties of 3D cell-seeded constructs [32, 40]. Controlled mechanical loading as part of post-surgical rehabilitation may serve as a viable strategy to further enhance the compressive moduli of

the remodeling hydrogels [40, 41]. Additional improvements in initial material properties of GelMA constructs may also be realized by adding exogenous hyaluronic acid and/or modifying the decellularization process so as to retain a higher endogenous sGAG content within the resulting ECM extracts [42]. As demonstrated by Levett et al. [38], supplementation of GelMA hydrogels with exogenous hyaluronic acid, rather than endogenous production by encapsulated cells, produced the greatest improvements in compressive mechanical properties.

While preservation of the bioactive physical and biochemical motifs of the native ECM is presumed to most faithfully reconstitute tissue-specific cell phenotypes, limitations in whole meniscus decellularization, as described in the Introduction, necessitate further processing to improve cell infiltration [43]. To that end, one must balance the disruption of native bioactive motifs with technical and biological utility gained by further ECM processing. Retention of higher sGAG content within ECM extracts may not only improve mechanical properties of constructs but may also enhance chondrogenic differentiation of seeded cells. For instance, hyaluronan of native ECM, through binding to the CD44 receptor of the cell surface, can upregulate chondrogenesis [44, 45]. Similarly, greater retention of soluble meniscal ECM through functionalization of the GelMA backbone (e.g., with heparin-binding domains) or covalent binding with methacrylated ECM proteins might bolster the chondrogenic effect of the hydrogels by prolonging cell-ECM interactions [27]. Alternatively, exogenous hyaluronan/sGAG could be added to the present formulation of ECM-supplemented GelMA for possible benefit. Nevertheless, future investigations elucidating the essential elements of the meniscus ECM that govern cell phenotype are essential to guide tissue engineering applications aimed at restoring the structure and function of the meniscus, in turn preserving joint integrity.

Therapeutic translation also requires consideration of how the hydrogel will be delivered in a surgical context. The current formulation of GelMA, with inclusion of a visible light-responsive photoinitiator, undergoes gelation in seconds, with complete curing in minutes [23]. A large animal study is currently ongoing in which autologous stromal cells are isolated from infrapatellar fat, suspended in a GelMA hydrogel containing TGF-β3 and soluble ECM, and photocrosslinked within a meniscal lesion concomitantly repaired with sutures, providing a point-of-care strategy for cell-based meniscal regeneration. With improvements in mechanical properties and the ability to adhere to native meniscal tissue, MSC-seeded hydrogels may be used to replace larger defects, similar to a related study investigating 3D printing protein-releasing polymeric scaffolds [46]. Assuming these material properties can be achieved, the cell-seeded photocrosslinkable hydrogel could serve as a dynamic biomaterial to restore meniscus structure in a single surgical procedure.

5. Conclusion

In this study, urea-extracted preparations of decellularized inner and outer meniscal ECM enhanced proliferation and fibrochondrogenic differentiation of 2D cultures of human bone marrow MSCs. GelMA hydrogels supplemented with soluble ECM fractions accelerated chondrogenic differentiation of seeded MSCs as determined by analyses of gene expression, protein deposition, and biochemical composition of the constructs. imECM supplementation

promoted early chondrogenic upregulation but was equivalent to omECM by later time points. While ECM supplementation alone enhanced chondrogenic differentiation, robust effects required supplementation of media with exogenous TGF-β3, which may have saturated the chondrogenic bioactivity of soluble ECM by day 42. Given these findings, photocrosslinkable hydrogels enhanced with meniscal ECM, TGF-β3, and MSCs, may offer a potential therapeutic strategy to promote meniscus neotissue formation when combined with surgical repair of meniscus tears.

Acknowledgments

The authors would like to thank Dr. Hang Lin and Mr. Aaron Sun for the provision of GelMA, and Dr. Jian Tan for MSC isolation and characterization.

Funding

This work was supported by the Department of Defense (grant no.W81XWH-15-1-0104). Benjamin B. Rothrauff is a pre-doctoral trainee supported by an NIH Training Grant (grant no. 5T32 EB001026]). Dr. Riccardo Gottardi was supported by the Ri.MED Foundation, Palermo, Italy.

References

1. Fox AJS, Wanivenhaus F, Burge AJ, Warren RF, Rodeo SA. The human meniscus: A review of anatomy, function, injury, and advances in treatment. Clin Anat. 2015; 28(2):269–287. [PubMed: 25125315]
2. Makris EA, Hadidi P, Athanasiou KA. The knee meniscus: Structure-function, pathophysiology, current repair techniques, and prospects for regeneration. Biomaterials. 2011; 32(30):7411–7431. [PubMed: 21764438]
3. Nakano T, Dodd CM, Scott PG. Glycosaminoglycans and proteoglycans from different zones of the porcine knee meniscus. J Orthop Res. 1997; 15(2):213–220. [PubMed: 9167623]
4. Di Giancamillo A, Deponti D, Addis A, Domeneghini C, Peretti GM. Meniscus maturation in the swine model: Changes occurring along with anterior to posterior and medial to lateral aspect during growth. J Cell Mol Med. 2014; 18(10):1964–74. [PubMed: 25216283]
5. Zhang X, Aoyama T, Ito A, Tajino J, Nagai M, Yamaguchi S, Iijima H, Kuroki H. Regional comparisons of porcine menisci. J Orthop Res. 2014; 32(12):1602–11. [PubMed: 25196310]
6. Vanderploeg EJ, Wilson CG, Imler SM, Ling CHY, Levenston ME. Regional variations in the distribution and colocalization of extracellular matrix proteins in the juvenile bovine meniscus. J Anat. 2012; 221(2):174–186. [PubMed: 22703476]
7. Coluccino L, Peres C, Gottardi R, Bianchini P, Athanassiou A, Diaspro A, Ceseracciu L. Anisotropic viscoelastic biomechanical mapping of knee meniscus cartilage. J Appl Biomater Funct Mater. 2016
8. Arnoczky SP, Warren RF. The microvasculature of the meniscus and its response to injury – an experimental study in the dog. Am J Sports Med. 1983; 11(3):131–141. [PubMed: 6688156]
9. Upton ML, Chen J, Setton LA. Region-specific constitutive gene expression in the adult porcine meniscus. J Orthop Res. 2006; 24(7):1562–1570. [PubMed: 16732608]
10. Rao AJ, Erickson BJ, Cvetanovich GL, Yanke AB, Bach BR Jr, Cole BJ. The meniscus-deficient knee biomechanics, evaluation, and treatment options, Orthop. J Sports Med. 2015; 3(10): 2325967115611386.
11. Fairbank TJ. Knee joint changes after meniscectomy. J Bone Jt Surg (Br). 1948; 30(4):664–670.
12. Rongen JJ, van Tienen TG, van Bochove B, Grijpma DW, Buma P. Biomaterials in search of a meniscus substitute. Biomaterials. 2014; 35(11):3527–3540. [PubMed: 24477194]
13. Marsano A, Wendt D, Raiteri R, Gottardi R, Stolz M, Wirz D, Daniels AU, Salter D, Jakob M, Quinn TM, Martin I. Use of hydrodynamic forces to engineer cartilaginous tissues resembling the

non-uniform structure and function of meniscus. Biomaterials. 2006; 27(35):5927–5934. [PubMed: 16949667]

14. Lakes EH, Matuska AM, McFetridge PS, Allen KD. Mechanical integrity of a decellularized and laser drilled medial meniscus. J Biomech Eng. 2016; 138(3):4032381. [PubMed: 26720513]
15. Chen YC, Chen RN, Jhan HJ, Liu DZ, Ho HO, Mao Y, Kohn J, Sheu MT. Development and characterization of acellular extracellular matrix scaffolds from porcine menisci for use in cartilage tissue engineering. Tissue Eng Part C. 2015; 21(9):971–986.
16. Stapleton TW, Ingram J, Fisher J, Ingham E. Investigation of the regenerative capacity of an acellular porcine medial meniscus for tissue engineering applications. Tissue Eng Part A. 2011; 17(1–2):231–242. [PubMed: 20695759]
17. Schwarz S, Koerber L, Elsaesser AF, Goldberg-Bockhorn E, Seitz AM, Durselen L, Ignatius A, Walther P, Breiter R, Rotter N. Decellularized cartilage matrix as a novel biomatrix for cartilage tissue-engineering applications. Tissue Eng Part A. 2012; 18(21–22):2195–2209. [PubMed: 22690787]
18. Wu J, Ding Q, Dutta A, Wang Y, Huang Y-h, Weng H, Tang L, Hong Y. An injectable extracellular matrix derived hydrogel for meniscus repair and regeneration. Acta Biomater. 16(2015):49–59.
19. Lin H, Yang G, Tan J, Tuan RS. Influence of decellularized matrix derived from human mesenchymal stem cells on their proliferation, migration and multi-lineage differentiation potential. Biomaterials. 2012; 33(18):4480–4489. [PubMed: 22459197]
20. Zhang YY, He YJ, Bharadwaj S, Hammam N, Carnagey K, Myers R, Atala A, Van Dyke M. Tissue-specific extracellular matrix coatings for the promotion of cell proliferation and maintenance of cell phenotype. Biomaterials. 2009; 30(23–24):4021–4028. [PubMed: 19410290]
21. Yang G, Rothrauff BB, Lin H, Gottardi R, Alexander PG, Tuan RS. Enhancement of tenogenic differentiation of human adipose stem cells by tendon-derived extracellular matrix. Biomaterials. 2013; 34(37):9295–9306. [PubMed: 24044998]
22. Shimomura K, Rothrauff BB, Tuan RS. Region-specific effect of decellularized meniscus extracellular matrix on mesenchymal stem cell-based meniscus tissue engineering. Am J Sports Med (Accepted).
23. Lin H, Cheng AWM, Alexander PG, Beck AM, Tuan RS. Cartilage tissue engineering application of injectable gelatin hydrogel with in situ visible-light-activated gelation capability in both air and aqueous solution. Tissue Eng Part A. 2014; 20(17–18):2402–11. [PubMed: 24575844]
24. Lin H, Zhang DN, Alexander PG, Yang G, Tan J, Cheng AWM, Tuan RS. Application of visible light-based projection stereolithography for live cell-scaffold fabrication with designed architecture. Biomaterials. 2013; 34(2):331–339. [PubMed: 23092861]
25. Keane TJ, DeWard A, Londono R, Saldin LT, Castleton AA, Carey L, Nieponice A, Lagasse E, Badylak SF. Tissue-specific effects of esophageal extracellular matrix. Tissue Eng Part A. 2015; 21(17–18):2293–2300. [PubMed: 26192009]
26. Wolf MT, Daly KA, Brennan-Pierce EP, Johnson SA, Carruthers CA, D'Amore A, Nagarkar SR, Velankar SS, Badylak SF. A hydrogel derived from decellularized dermal extracellular matrix. Biomaterials. 2012; 33(29):7028–7038. [PubMed: 22789723]
27. Visser J, Levett PA, te Moller NCR, Besems J, Boere KWM, van Rijen MHP, de Grauw JC, Dhert WJA, van Weeren PR, Malda J. Crosslinkable hydrogels derived from cartilage, meniscus, and tendon tissue. Tissue Eng Part A. 2015; 21(7–8):1195–1206. [PubMed: 25557049]
28. Nichol JW, Koshy ST, Bae H, Hwang CM, Yamanlar S, Khademhosseini A. Cell-laden microengineered gelatin methacrylate hydrogels. Biomaterials. 2010; 31(21):5536–5544. [PubMed: 20417964]
29. Almeida HV, Eswaramoorthy R, Cunniffe GM, Buckley CT, O'Brien FJ, Kelly DJ. Fibrin hydrogels functionalized with cartilage extracellular matrix and incorporating freshly isolated stromal cells as an injectable for cartilage regeneration. Acta Biomater. 2016; 36:55–62. [PubMed: 26961807]
30. Almeida HV, Liu YR, Cunniffe GM, Mulhall KJ, Matsiko A, Buckley CT, O'Brien FJ, Kelly DJ. Controlled release of transforming growth factor-beta 3 from cartilage-extra-cellular-matrix-derived scaffolds to promote chondrogenesis of human-joint-tissue-derived stem cells. Acta Biomater. 2014; 10(10):4400–4409. [PubMed: 24907658]

31. Muhammad H, Schminke B, Bode C, Roth M, Albert J, von der Heyde S, Rosen V, Miosge N. Human migratory meniscus progenitor cells are controlled via the tgf-beta pathway. Stem Cell Reports. 2014; 3(5):789–803. [PubMed: 25418724]
32. Puetzer JL, Bonassar LJ. Physiologically distributed loading patterns drive the formation of zonally organized collagen structures in tissue engineered meniscus. Tissue Eng Part A. 2016; 22(13–14): 907–916. [PubMed: 27245484]
33. Nerurkar NL, Han WJ, Mauck RL, Elliott DM. Homologous structure-function relationships between native fibrocartilage and tissue engineered from msc-seeded nanofibrous scaffolds. Biomaterials. 2011; 32(2):461–468. [PubMed: 20880577]
34. Fisher MB, Henning EA, Soeegaard N, Bostrom M, Esterhai JL, Mauck RL. Engineering meniscus structure and function via multi-layered mesenchymal stem cell-seeded nanofibrous scaffolds. J Biomech. 2015; 48(8):1412–1419. [PubMed: 25817333]
35. Baek J, Chen X, Sovani S, Jin S, Grogan SP, D'Lima DD. Meniscus tissue engineering using a novel combination of electrospun scaffolds and human meniscus cells embedded within an extracellular matrix hydrogel. J Orthop Res. 2015; 33(4):572–583. [PubMed: 25640671]
36. Fithian DC, Kelly MA, Mow VC. Material properties and structure-function relationships in the menisci. Clin Orthop Relat Res. 252(1990):19–31.
37. Proctor CS, Schmidt MB, Whipple RR, Kelly MA, Mow VC. Material properties of the normal medial bovine meniscus. J Orthop Res. 1989; 7(6):771–782. [PubMed: 2677284]
38. Levett PA, Hutmacher DW, Malda J, Klein TJ. Hyaluronic acid enhances the mechanical properties of tissue-engineered cartilage constructs. Plos One. 2014; 9(12):e113216. [PubMed: 25438040]
39. Puetzer JL, Bonassar LJ. High density type i collagen gels for tissue engineering of whole menisci. Acta Biomater. 2013; 9(8):7787–7795. [PubMed: 23669622]
40. Bian L, Zhai DY, Zhang EC, Mauck RL, Burdick JA. Dynamic compressive loading enhances cartilage matrix synthesis and distribution and suppresses hypertrophy in hmsc-laden hyaluronic acid hydrogels. Tissue Eng Part A. 2012; 18(7–8):715–724. [PubMed: 21988555]
41. Ambrosio F, Wolf SL, Delitto A, Fitzgerald GK, Badylak SF, Boninger ML, Russell AJ. The emerging relationship between regenerative medicine and physical therapeutics. Phys Ther. 2010; 90(12):1807–1814. [PubMed: 21030663]
42. Elder BD, Eleswarapu SV, Athanasiou KA. Extraction techniques for the decellularization of tissue engineered articular cartilage constructs. Biomaterials. 2009; 30(22):3749–3756. [PubMed: 19395023]
43. Crapo PM, Gilbert TW, Badylak SF. An overview of tissue and whole organ decellularization processes. Biomaterials. 2011; 32(12):3233–3243. [PubMed: 21296410]
44. Bian L, Guvendiren M, Mauck RL, Burdick JA. Hydrogels that mimic developmentally relevant matrix and n-cadherin interactions enhance msc chondrogenesis. Proc Natl Acad Sci. 2013; 110(25):10117–10122. [PubMed: 23733927]
45. Carrion B, Souzanchi MF, Wang VT, Tiruchinapally G, Shikanov A, Putnam AJ, Coleman RM. The synergistic effects of matrix stiffness and composition on the response of chondroprogenitor cells in a 3d precondensation microenvironment. Adv Healthc Mater. 2016; 5(10):1192–202. [PubMed: 26959641]
46. Lee CH, Rodeo SA, Fortier LA, Lu C, Erisken C, Mao JJ. Protein-releasing polymeric scaffolds induce fibrochondrocytic differentiation of endogenous cells for knee meniscus regeneration in sheep. Sci Transl Med. 2014; 6(266):266ra171.

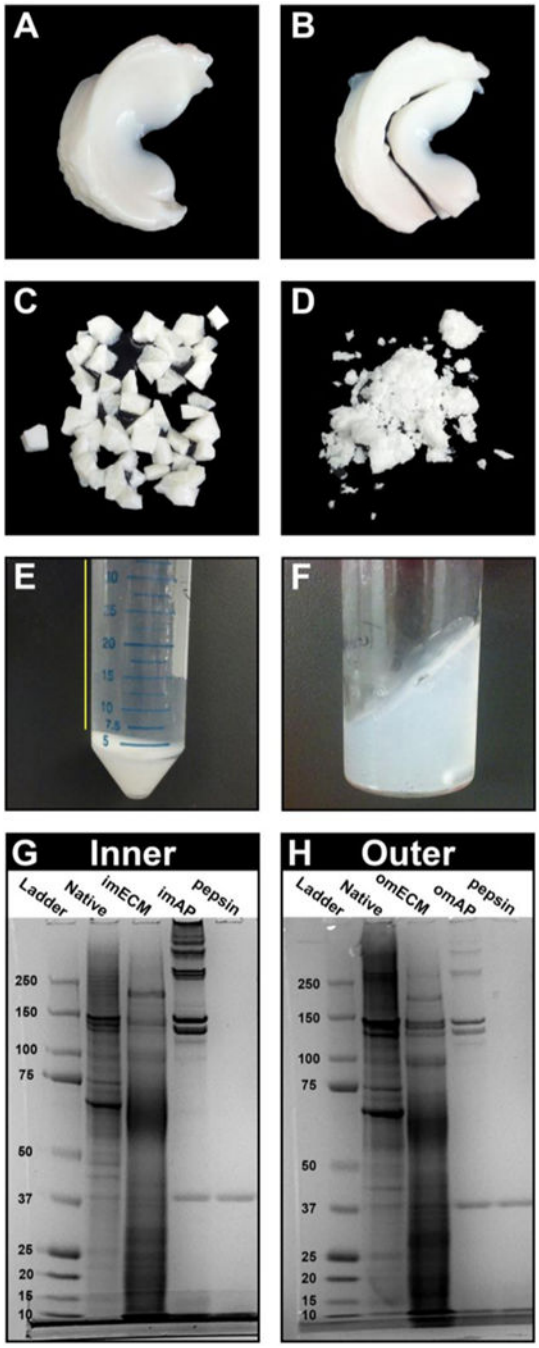

Fig. 1.

Solubilization of ECM from inner and outer meniscus. (A) Whole menisci were obtained from 6–8 week old cow hindlimbs, (B) halved, and (C) manually minced (8–27 mm^3). Following decellularization, (D) tissues were cryomilled and soluble fractions were obtained either by (E) urea-extraction (supernatant was retained, yellow line) or (F) acid-pepsin digestion. SDS-PAGE of (G) inner meniscus and (H) outer meniscus tissues and soluble preparations demonstrate that urea extraction (imECM, omECM) retained low and moderate molecular weight proteins while pepsin digestion (imAP, omAP) yielded mostly collagen.

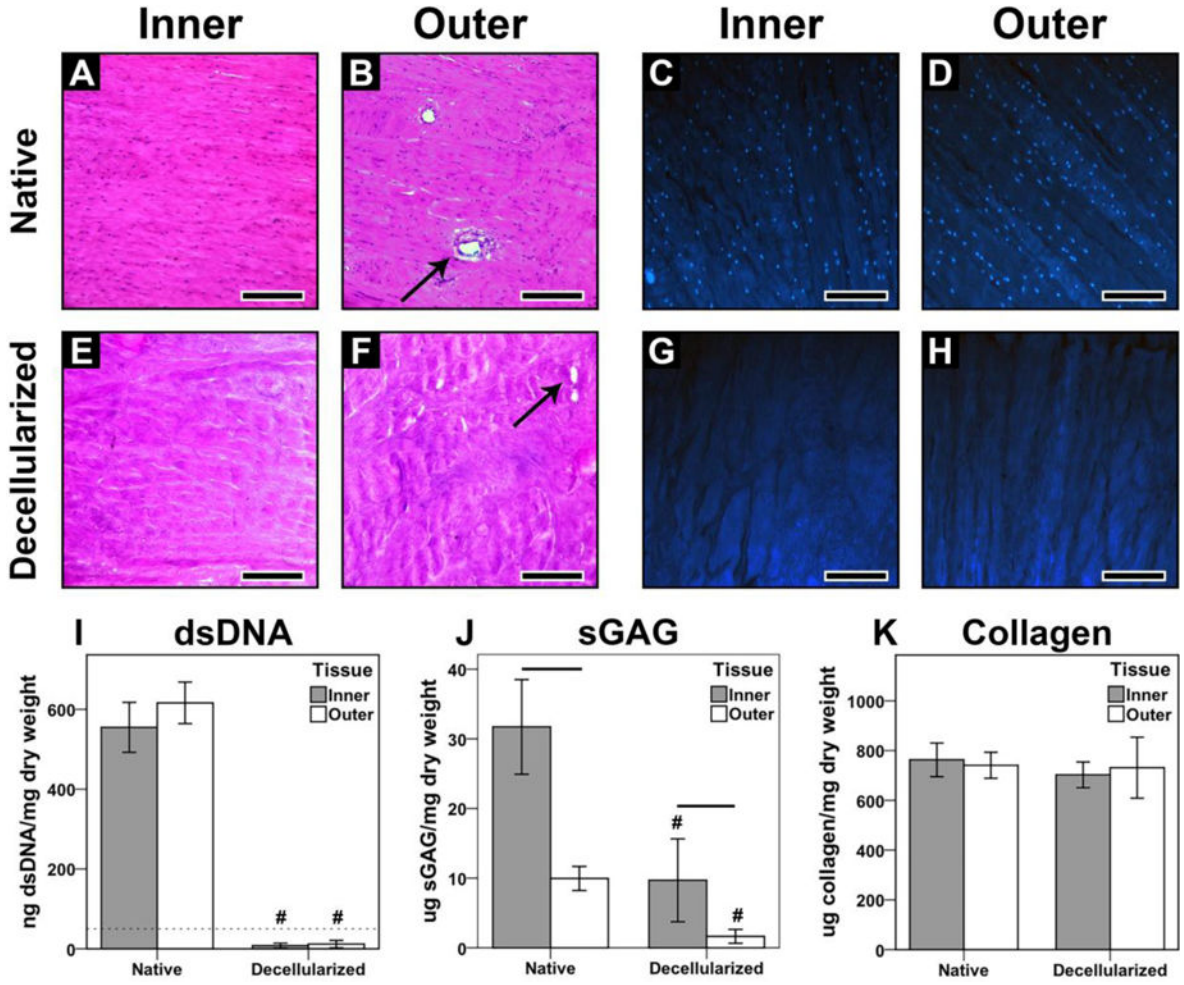

Fig. 2.

Characterization of native and decellularized meniscus tissue. (A, B) H&E and (C, D) DAPI staining of native inner and outer meniscus, respectively. (E, F) H&E and (G, H) DAPI staining of decellularized tissues. Arrows indicate blood vessels found in outer meniscus (B, F); Scale bar = 500 μm. (I) dsDNA content of native and decellularized meniscus; dotted line at 50 ng/mg is established threshold for sufficient decellularization [43]. (J) Total sGAG content. (K) Total collagen content. For biochemical assays, n = 8–10 per condition. # $p < 0.001$, significant difference between native and decellularized tissue from a given region. Lines over bars indicate significant difference between regions for a given step, $p < 0.05$.

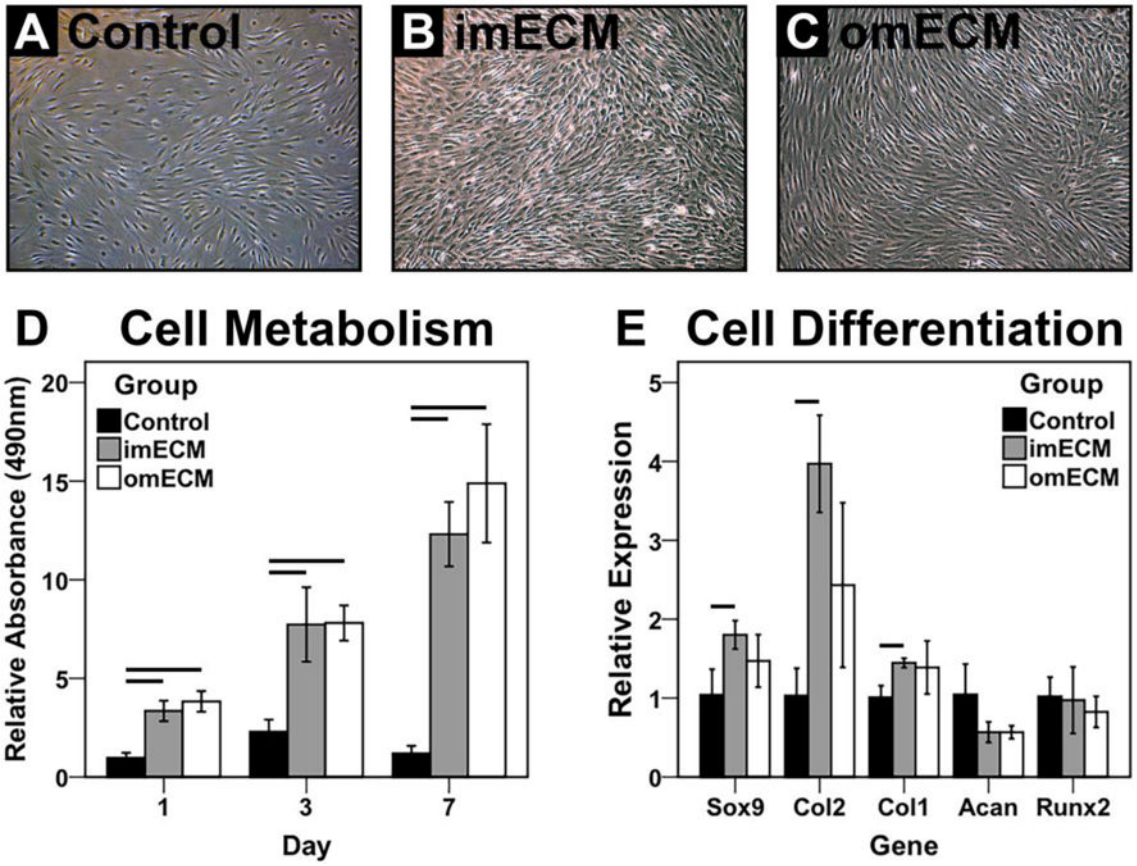

Fig. 3.

Bioactivity of soluble ECM extracts on MSCs in 2D culture. (A–C) Phase contrast microscopy; Scale bar = 100 μm. (D) MTS assay measuring cell metabolism as a function of culture time; n = 6–8 per condition; Lines indicate significant difference between groups on given day, $p < 0.05$. (E) Gene expression analysis on day 3; n=3 independent trials, each performed in biological triplicate; Lines indicate significant difference between groups, $p < 0.05$.

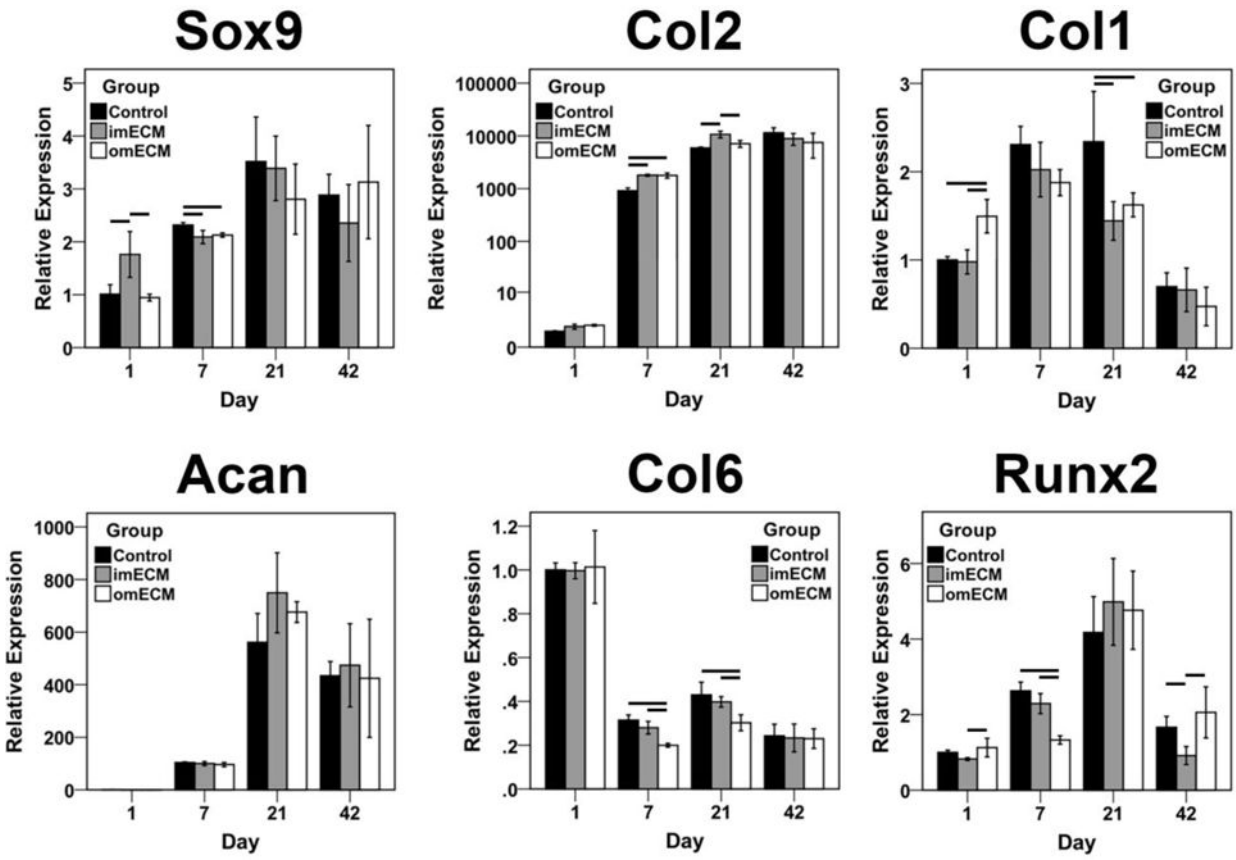

Fig. 4.

Gene expression analysis of 3D MSC-GelMA constructs as a function of culture time. Relative expression normalized to day 1 Controls. n=3 independent trials, each performed in biological triplicate; Lines indicate significant differences between groups, $p < 0.05$.

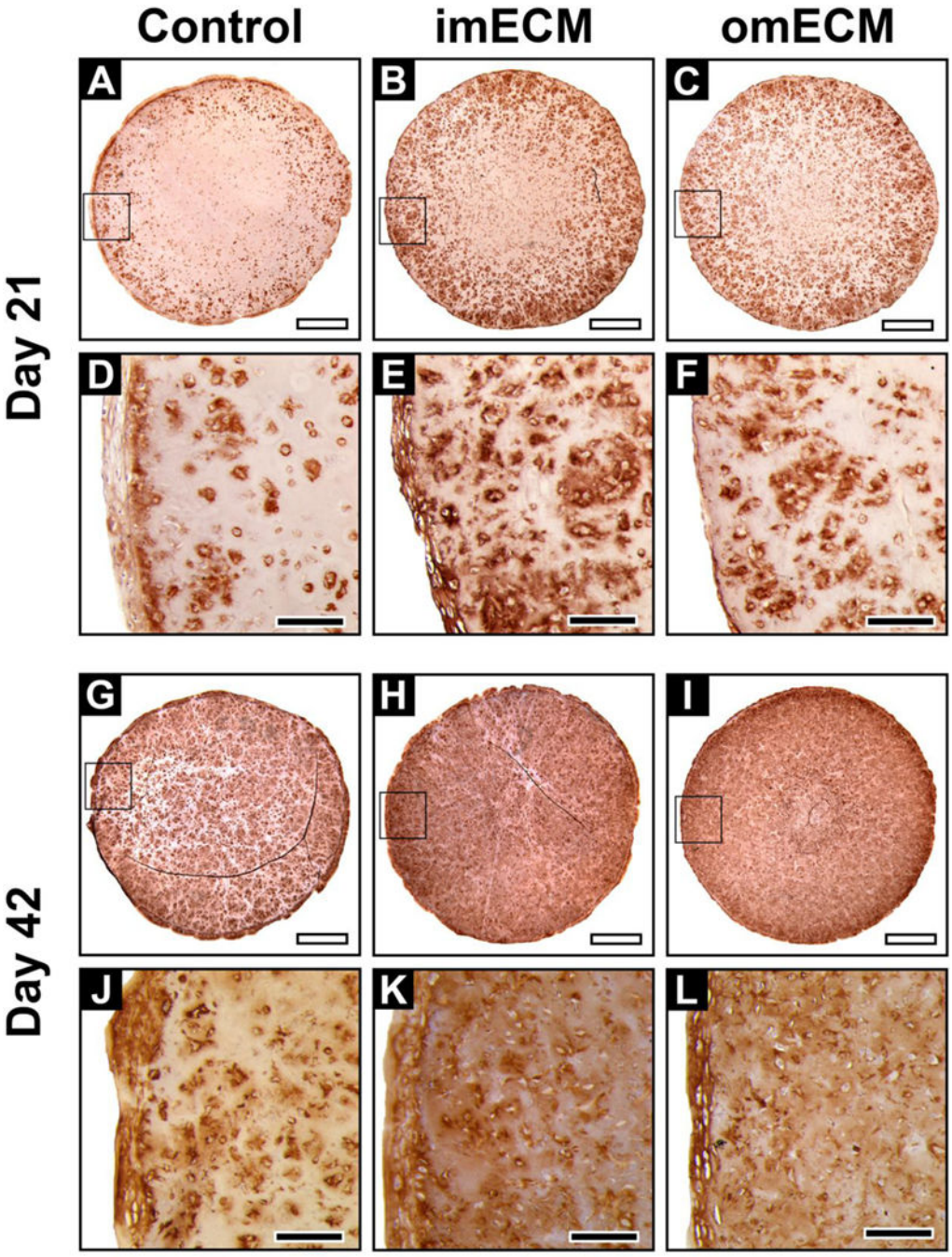

Fig. 5.

Immunohistochemical staining of collagen type II in 3D MSC-seeded GelMA constructs. (A–F) Constructs on day 21; (A–C) Low magnification, scale bar = 1 mm; Area of magnification shown by black box; (D–F) High magnification, scale bar = 200 μm. (G–L) Constructs on day 42; (G–I) Low magnification, scale bar = 1 mm; Area of magnification shown by black box; (J–L) High magnification, scale bar = 200 μm.

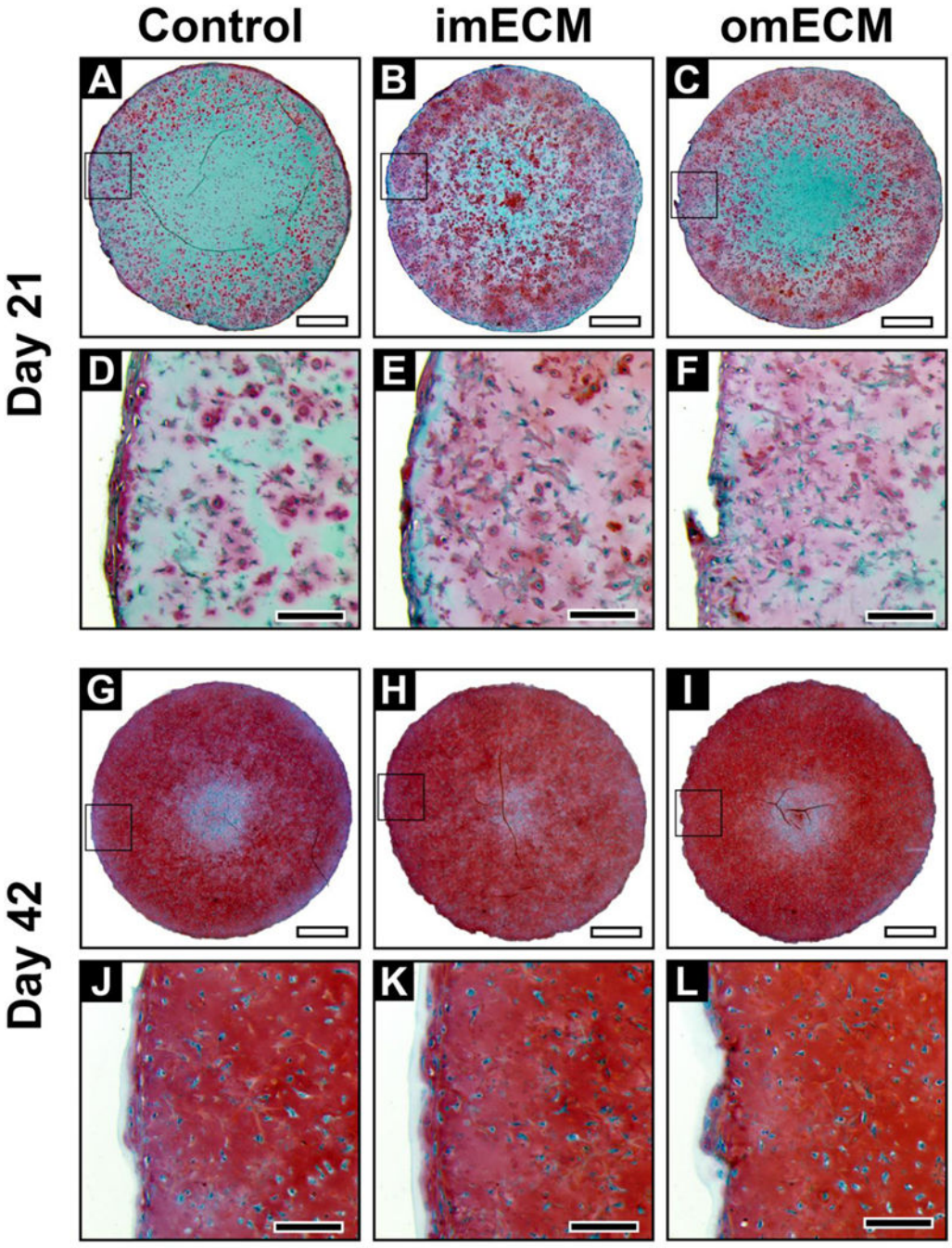

Fig. 6.

Safranin O staining of 3D MSC-seeded GelMA constructs. (A–F) Constructs on day 21; (A–C) Low magnification, scale bar = 1 mm; Area of magnification shown by black box; (D–F) High magnification, scale bar = 200 μm. (G–L) Constructs on day 42; (G–I) Low magnification, scale bar = 1 mm; Area of magnification shown by black box; (J–L) High magnification, scale bar = 200 μm.

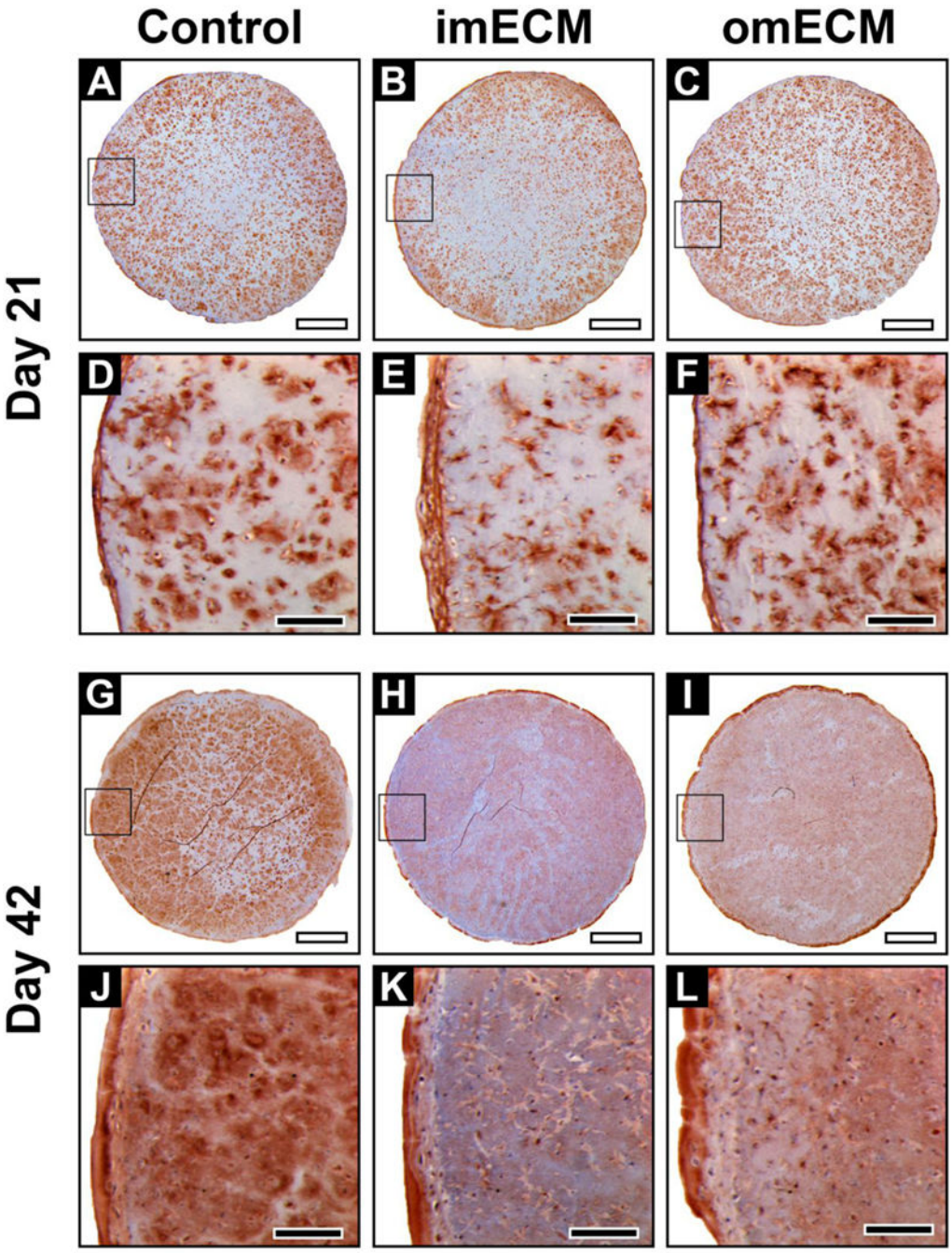

Fig. 7.

Immunohistochemical staining of collagen type I in 3D MSC-seeded GelMA constructs. (A–F) Constructs on day 21; (A–C) Low magnification, scale bar = 1 mm; Area of magnification shown by black box; (D–F) High magnification, scale bar = 200 μm. (G–L) Constructs on day 42; (G–I) Low magnification, scale bar = 1 mm; Area of magnification shown by black box; (J–L) High magnification, scale bar = 200 μm.

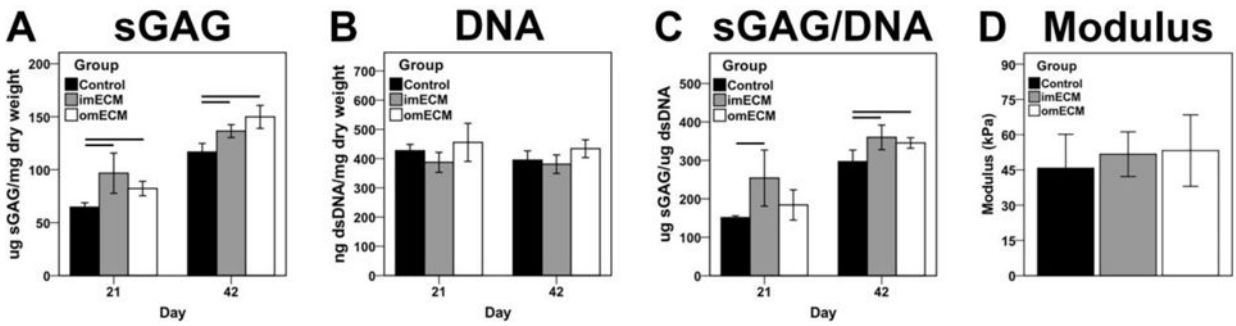

Fig. 8.

Biochemical composition (days 21 and 42) and compressive modulus (day 42) of 3D MSC-seeded GelMA constructs. (A) Total sGAG content. (B) Total dsDNA content. (C) sGAG normalized by DNA. (D) Compressive modulus on day 42. n=8–10 samples per condition; Lines indicate significant difference between groups, $p < 0.05$.

Table 1

Growth factor and cytokine concentrations (pg/ml) measured in imECM and omECM

Protein	imECM	omECM
bFGF	0.0	362.6
EGF R	3.1	0.0
EG-VEGF	0.1	0.0
IGFBP-4	3.6	0.0
Insulin	0.0	36.6
NT-3	3.4	3.2
OPG	59.0	54.7
SCF	1.8	1.1
SCF R	16.3	0.0
TGFb1	241.7	140.9
TGFb3	29.3	0.0